

Received January 14, 2019, accepted February 13, 2019, date of publication March 7, 2019, date of current version March 18, 2019.

Digital Object Identifier 10.1109/ACCESS.2019.2901959

Move Your Body: Age Estimation Based on Chest Movement During Normal Walk

QAISER RIAZ^{ID¹}, MUHAMMAD ZEESHAN UL HASNAIN HASHMI¹, MUHAMMAD ARSLAN HASHMI¹, MUHAMMAD SHAHZAD¹, HASSAN ERRAMI², AND ANDREAS WEBER²

¹Department of Computing, School of Electrical Engineering and Computer Science, National University of Sciences and Technology, Islamabad 44000, Pakistan

²Department of Computer Science II, University of Bonn, 53113 Bonn, Germany

Corresponding author: Qaiser Riaz (qaiser.riaz@seecs.nust.edu.pk)

ABSTRACT The estimation of soft biometrics of a subject, including age, through the gait analysis is a challenging area of research due to variations in individuals' gaits and the effect of ageing on gait patterns. In this paper, we present the results of age estimation based on the analysis of inertial data of human walk. We have recorded 6D accelerations and angular velocities of 86 subjects while performing standardized gait tasks using chest-mounted inertial measurement units. The recorded data were segmented to decompose the long sequences of signals into single steps. For each step, we compute a total of 50 spatio-spectral features from 6D components. We trained three different machine learning classifiers—random forests, support vector machines, and multi-layer perceptron—to estimate the human age. Two different types of cross validation strategies, i.e., tenfold and subjectwise cross validation were employed to gauge the performance of the estimators. The results reveal that it is possible to predict the age of a subject with higher accuracy. With a random forest regressor, when trained and validated on hybrid data, we achieved an average root mean square error of 3.32 years and a mean absolute error of 1.75 years under tenfold cross validation and average root mean square error of 8.22 years under subjectwise cross validation. Since our participants belong to two different demographical regions, i.e., Europe and South Asia, we confirm on broader empirical basis previous findings that age information is present in the human gait. Our proposed approach allows rather robust estimations of age based on the inertial data of a single step, as the used data consist of those collected on different ground surfaces, and the participants were also told to walk pretending different emotional states. The findings on the existing data point out the change of gait while aging, which will also imply that person identification using the gait depends on data that is not too old.

INDEX TERMS Age estimation, inertial sensor based age estimation, human gait analysis, smartphone and wearable, soft biometrics.

I. INTRODUCTION

Human gait provides valuable biometric signature particularly in uncontrolled scenarios and is of great practical interest especially when it comes to applications related to intelligent monitoring/surveillance. Moreover, since the walking style of person varies from one another, the human gait is believed to be unique [1]. This has attracted attention of many researchers and various approaches related to gait-based human identification [2], [3], gender classification [4]–[6], and age estimation [4], [7], [8] have been proposed over the last decade. Particularly, human age estimation has wide

The associate editor coordinating the review of this manuscript and approving it for publication was Bora Onat.

range of applications including forensics, surveillance and law enforcement, legal systems, human-computer interaction, recommendation systems and many more. Typically, the age estimation is accomplished in two sequential steps where in the first step the important features (e.g., anthropometric model [9], local binary patterns [10] etc.) are discriminatively extracted/represented while in the second step these features are utilized for age estimation by employing a regression [11] or classification [4] model. Although these approaches work fairly well for image-based gait analysis but are also subjected to problems related to 3D to 2D projective geometry, occlusions, scale etc. These issues consequently pose limitations in precise motion representation and thus consequently lead to inaccurate estimation of characteristic

gait information. Use of active or passive sensors/devices allow to rectify the aforementioned problems by directly capturing the accurate motion data which helps in effective motion pattern analysis and to extract kinematics properties needed for meaningful gait analysis for precise age estimation.

Recently, the market of wearable devices has grown significantly [12], [13]. The availability of large number of such sensors [14] reflects that there is an increasingly growing interest to capture/analyze the human motion for various applications. Although in comparison to modern motion capture sensors [15], [16], the data provided by these sensors (i.e., using tri-axial accelerometers) may be less accurate, many techniques have been proposed to reconstruct the human motion [17] and classify soft biometrics [18], [19] even with sparse sensor setups. Another promising aspect and low-cost solution to capture the motion data is with the help of smartphones. These devices are usually equipped with an in-built tri-axial accelerometer and has been shown in reliable estimation of human gait [20], number of steps [21], and stride-to-stride interval [22].

In this research activity, we explored the possibility of estimating human age via gait analysis using the inertial measurement units (IMUs) data including accelerometer and gyroscope. In this regard, we specifically utilized two different types of devices to capture the inertial data: (1) smartphone embedded IMU (MPU-6500) and (2) wearable IMU (APDM Opal). The reason behind this is to analyze and validate the performance of the proposed approach on the recorded data using two different sensor modalities. In total, we collected the data from 86 participants which includes 49 males and 37 females with ages ranging from 17 to 72 years. The proposed approach is capable of processing single steps inertial data from both of the sensors. The data signals are primarily segmented into single steps and different statistical/spectral features are extracted for each respective step. For the classification/regression task, the computed features are utilized to perform inference/prediction using supervised machine learning algorithms. Specifically, we employed random forests (RF) that is based on aggregation of multiple decision trees, support vector machine (SVM) for discriminative learning, and multilayer perceptron (MLP) to perform the age estimation using feed forward neural networks. In sum, our experiments demonstrate that it is indeed possible to estimate human age reliably and accurately by gait analysis using the inertial sensors data. As our participants belong to two different demographical regions i.e. Europe and South-Asia, we confirm on a broader empirical basis previous findings that age information is present in human gait. Our proposed approach allows rather robust estimations of age based on inertial data of a single step, as the used data consists of those collected on different group surfaces, and the participants were also told to walk pretending different emotional states.

The rest of the paper is organized as follows: Section II reviews the related work on age estimation. Section III

describes our methodology: population characteristics, sensor placement, data collection, pre-processing, signal decomposition and features extraction. Section IV presents results of age estimation obtained using individual as well as hybrid sensors. Section V provides a discussion on results. Finally, in Section VI, the conclusion is drawn and the future perspectives are discussed.

II. RELATED WORK

Approaches employing gait analysis to estimate human age may be grouped into two categories i.e., techniques processing either the visual image(s) [11], [23]–[27] or non-visual (usually inertial [4], [17], [18]) data. In the case of vision-based gait analysis, the presented approaches usually learn gait signatures by analyzing the temporal sequence of (person) contour lines or silhouettes. Such analysis yields a gait representation that translates the temporal sequence into a 2D periodic pattern [28]. Over the last decade, several gait analysis methods employing visual data for estimating soft biometric including human age have been proposed. For instance, Lu *et al.* [8] used background subtraction to extract person silhouettes and later employed sparse reconstruction based metric learning to enhance the discriminative feature extraction. Similarly, Nabilah *et al.* [29] analyzed both the spatio-temporal traverse and longitudinal silhouette projections within a gait cycle for human age estimation. To enhance the gait characteristics, Lu and Tan [7] utilized a complete set of extracted Gabor features to estimate person age.

In the context of gait analysis using inertial (or non-visual) data, a common strategy is to utilize one or more inertial measurement unit(s) to record gait patterns for the estimation of soft biometrics. For this purpose, Sabatini *et al.* [30] employed IMU to collect gait samples for human age estimation. Ellis *et al.* [31] utilized multiple IMUs mounted at hip and wrists for data collected to characterize human physical activities. Mannini and Sabatini [32] also presented a method for classifying human activities using Hidden Markov Models (HMMs) and Gaussian Mixture Models (GMMs). In contrast to inertial sensors, Dobry *et al.* [33] proposed a technique based on GMM and support vector machine to estimate human age using speech input. Hoffmann *et al.* [34] described a method, in which gait patterns were extracted using sensor floor for estimation of person age. Tsimperidis *et al.* [35] used multi-layer perceptron to detect age by exploiting keystroke dynamics from authentication failures of user. An approach for predicting age, gender and height soft biometric has been presented, by utilizing on body IMU to record gait data by Riaz *et al.* [4]. With the rapid growth in the embedded devices supporting biometric technology (e.g., smartphones), there is an increasing trend in the estimation of soft biometrics using such devices. In this regard, Kelishomi *et al.* [36] uses smartphone motion data and perform user basic activity analysis to detect user age group, foot wear and floor surface types. Ahmed *et al.* [37], utilized on-board accelerometers and gyroscopes of smartphones to extract gait samples for predicting age groups and

body mass index. Other works using smartphones e.g., investigation of Parkinson's disease severity via behavior analysis, detection of user traits and demographics including age, and gait analysis have been presented in [20] and [38]–[40] respectively. Although the use of smartphones and other wearable devices for age estimation is still a relatively new and far less work has been done in demographic analysis compared to biometric authentication both in industry and academia [41], it has immense potential in enabling quick verification especially for surveillance/monitoring purposes.

Notice that in the context of facial image based age estimation, an array of methods have been developed to perform visual features (or image) based age estimation. For instance, Geng *et al.* [42] adopted facial aging signatures to estimate human age. Han *et al.* [43] performed human vs machine age estimation comparison by exploiting individual facial features. These conventional approaches mainly rely on representing discriminative handcrafted features contained in the visual face and thus require sophisticated methods for feature representation and architecture design. With the recent advancements and ability to learn features to model (non-linear) complex facial aging patterns, several deep learning based solutions have been developed recently. Among them, Wang *et al.* [44] presented the first age estimation results obtained by exploiting feature representations extracted using different layers of a convolution neural network (CNN). Kang *et al.* [26] employed a deep residual network to extract robust features to reduce the effects of motion blur and illumination changes. Yoo *et al.* [23] employed a multi-task deep learning method to enhance estimation of human age by taking into account the auxiliary tasks, i.e., gender recognition, while predicting a discrete age value. Similarly, Levi and Hassner [45] also adopted CNN to perform age estimation along with gender classification. Although deep learning solutions provide much better age estimates than compared to conventional handcrafted feature based approaches, a major bottleneck to these solutions is that they require a large amount of training data along with high computational resources. Moreover, the changes in facial characteristics with the gender, make-up etc., may cause the apparent age to significantly vary from the actual biological age, thus the use of facial images to predict human age remains highly challenging despite the accuracy improvements obtained by recent deep learning frameworks.

III. METHODOLOGY

In this section, we describe the architecture of the proposed approach for human age estimation. Our methodology consists of six essential steps: data collection, pre-processing of data to suppress noise and to find local minimas, decomposition of long sequence of signals into single steps using local minimas, extraction of spatio-temporal features, training estimators, and finally predicting age. In the following, we explain all of the components in detail.

A. PARTICIPANTS' CONSENT

The participants were all healthy volunteers who were briefed in detail about the nature and purpose of the experiments to be conducted in this research activity. They were also informed about the data privacy policy, the type and nature of the collected data, how the data will be used, and possible outcomes of the research. All of the willing participants were asked to sign a consent form by filling-in their particulars including name, gender, age, and height.

B. EXPERIMENT SETUPS AND CHARACTERISTICS OF THE POPULATION

The standardized gait tasks consisted of a similar approach as proposed in [4] i.e. walking straight on a 10-meter surface, turning around, and walking back to the starting point. The subjects repeated the standardized gait task twice resulting in a 4x10-meter walk. The data were collected under three different experiment setups namely Setup-A, Setup-B, and Setup-C. In Setup-A, the participants were told to walk pretending in one of the six different emotional states (happy, sad, angry, fear, surprise, disgust). In Setup-B, subjects were asked to walk naturally on six different surfaces (carpet, concrete floor, grass, road, soil and laminate tiles). The Setup-C consisted of a subset of gait dataset from our previous work [4]. In this setup, subjects were asked to walk on hard surface in their natural gait. In all of the experiments, the subjects were wearing shoes without any restriction to the type of shoes. The characteristics of the population for all three setups are shown in Table 1. The age and gender distribution of the population is presented in Fig. 1.

TABLE 1. Characteristics of the population considered in the study under different experiment setups. A smartphone's on-board IMU (MPU-6500) was used to collect data in Setup-A and Setup-B whereas an APMD Opal IMU was used to collect data in Setup-C.

	All Setups	Setup-A	Setup-B	Setup-C
Participants	86	40	20	26
Male:Female	49:37	26:14	11:9	12:14
Age (y, $\mu \pm \sigma$)	33.8 ± 14.8	25.2 ± 5.9	32.6 ± 13.7	48.1 ± 12.7
Height (cm, $\mu \pm \sigma$)	172.1 ± 8.9	171.6 ± 8.4	169.8 ± 7.9	174 ± 10.2

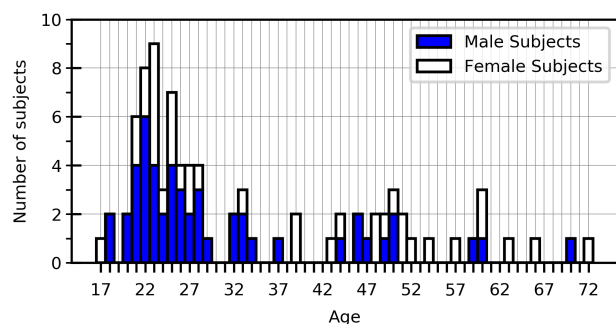


FIGURE 1. Age and gender distribution of the population.

TABLE 2. Technical specifications of the smartphone embedded MPU-6500 and APDM Opal IMU sensors.

	APDM Opal IMU		MPU-6500	
	Accelerometer	Gyroscope	Accelerometer	Gyroscope
Axes	3	3	3	3
Noise	$0.0012 \text{ m/s}^2/\sqrt{\text{Hz}}$	$0.05 \text{ deg/s}/\sqrt{\text{Hz}}$	$0.0029 \text{ m/s}^2/\sqrt{\text{Hz}}$	$0.01 \text{ deg/s}/\sqrt{\text{Hz}}$
Output Rate	20 to 128 Hz	20 to 128 Hz	5 to 100 Hz	5 to 100 Hz
Range	$\pm 2\text{g}$ or $\pm 6\text{g}$	$\pm 2000 \text{ deg/s}$	$\pm 2\text{g}$, $\pm 4\text{g}$, $\pm 8\text{g}$ or $\pm 16\text{g}$	$\pm 2000 \text{ deg/s}$
Resolution	14 bits	14 bits	16 bits	16 bits

C. SENSOR TYPES AND PLACEMENT

We have used two different types of sensors for data collection i.e. a smartphone embedded IMU (MPU-6500) [46] and a wearable IMU (APDM Opal) [47]. The reason of using two different sensor types is to evaluate the behavior of the proposed algorithm on two different sensor modalities. The android based smartphone, which is used to collect data for Setup-A and Setup-B, is equipped with an MPU-6500 MEMS to measure 6D accelerations and angular velocities. The wearable IMU, used in Setup-C, houses 3D accelerometers and 3D gyroscopes to measure 6D accelerations and angular velocities. Table 2 shows the technical specifications of MPU-6500 MEMS and APDM Opal IMU. A loosely attached sensor can introduce noise during data collection. To avoid this, the sensors were firmly and carefully attached on the chest of the subject using elastic bands as shown in Fig. 2.



FIGURE 2. The sensors were tightly attached on the chest using elastic bands. (left) Smartphone (MPU-6500) sensor, (right) APDM Opal IMU.

D. DATA COLLECTION

Three different types of experiments setups, as explained earlier, were used for data collection. Details of the experiments are:

- 1) The participants of Setup-A were asked to walk on hard surface with shoes on by considering themselves in one of the six basic emotions. The basic emotions included: *happy, sad, angry, fear, surprise, and disgust*. The participants performed the gait tasks for each of the emotions and hence ending up into 6 data collection sessions. A total of 40 South Asian subjects voluntarily participated and recorded their data.
- 2) The participants of Setup-B were asked to walk on six different surfaces with shoes on in their natural gait. The considered surfaces with variation in friction and hardness were *carpet, concrete floor, grass, road, soil and laminate tiles*. Hence, 6 data collection sessions for

each surface per participant were carried out. A total of 20 South Asian subjects voluntarily participated and recorded their data.

- 3) The participants of Setup-C were asked to walk on hard surface with shoes on. This dataset is a subset of the data from our previous work [4]. A total of 26 European subjects voluntarily participated and recorded their data.

E. PRE-PROCESSING

The output sampling rate of MPU-6500 MEMS sensor is adjustable between 20-100Hz. We have chosen a sampling rate of 75 Hz in our experiments. The data recorded under Setup-C was using APDM Opal IMU at a sampling rate of 128Hz. To match the sampling rate of all experiments, resampling was used to lower down the sampling rate from 128Hz to 75Hz using matlab's *resample* function. After achieving same sampling rate for all experiments, the next pre-processing task was to suppress noise. We used a moving average filter of window size 9 for noise suppression and smoothing of the signal as shown in Fig. 3 – Pre-processing.

F. SIGNAL DECOMPOSITION INTO SINGLE STEPS

The gait data produced by each experiment consists of long sequences of inertial signals generated by the bipedal locomotion of the subjects. These long sequences need to be decomposed into single steps. A well-known method of decomposing inertial signals into single steps is by means of detecting peaks (by finding local minimas) and valleys (by finding local maximas) in the input signal [48]–[50]. We have used valleys to segment the input signal into single steps (Fig. 3 – Pre-processing, Step Segmentation). The stride length differs from subject to subject because of variable walking speeds and gait characteristics of each subject. The difference in stride length leads to varying total number of frames in each step. The indexes of the valleys are computed on the y-component of accelerometer (which is in the direction of gravity) and same indexes are used to segment the remaining components of the accelerometer and gyroscope.

G. FEATURE EXTRACTION

Time and frequency domain features were computed for 6D components of all of the single steps (Fig. 3 – Features). Time domain features include mean, median, minimum and

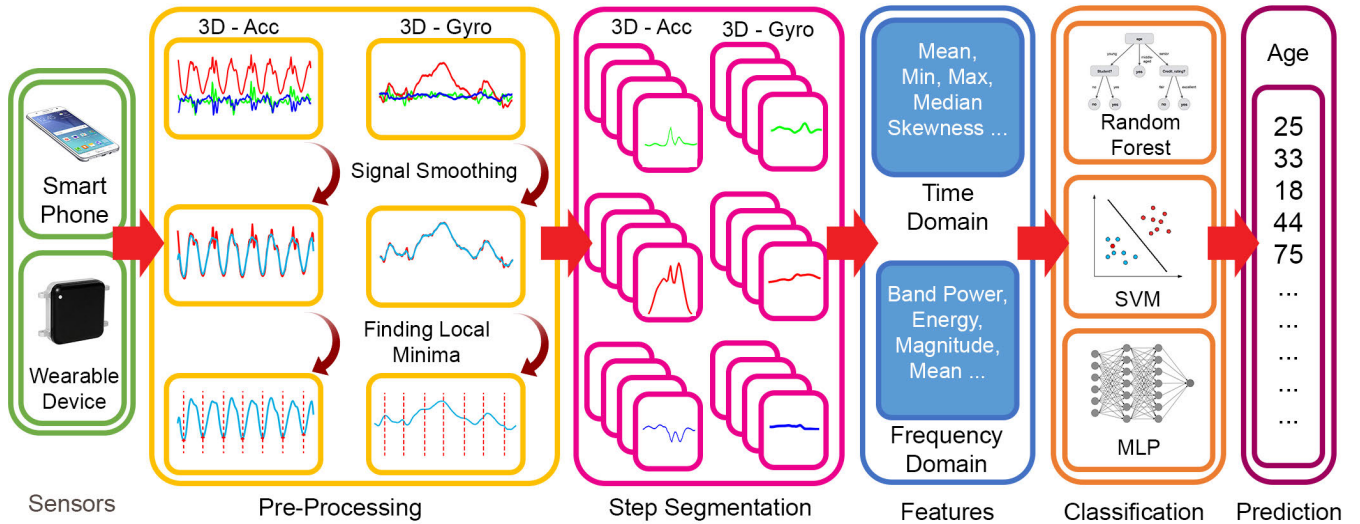


FIGURE 3. The general work-flow of the proposed method. The raw signals from 6D-components are smoothed and local minimas are computed in the pre-processing step, which are used to decompose signal into single steps. A variety of time and frequency domain features are computed and the estimators are trained and tested to predict age.

maximum value of step; indexes of minimum and maximum value; root mean square; mean absolute deviation; skewness; kurtosis; power; energy; entropy; inter-quartile range and signal magnitude area. Fast Fourier Transform (FFT) was used to calculate frequency domain features which include mean value of signal, magnitude, energy and band power of the signal. Initially, we computed 114 features of 6D components ($15 \times 6 = 90$ features from time domain and $4 \times 6 = 24$ features from frequency domain). However, with experiments we had found the top 50 features, using mean decrease impurity, which could produce more or less similar results as ones computed with full features set. The added benefit of top 50 features is lower processing needs. Table 3 describes the list of all features extracted from 6D single steps.

H. REGRESSION WITH MULTIPLE MODELS

The goal of the proposed age estimation algorithm is to learn the underlying patterns from the features set and estimate the age of a subject. Age being a continuous variable is a suitable candidate for regression. To perform regression, we trained the dataset using Support Vector Regressor, Random Forest Regressor, and Multi-Layer Perceptron.

1) RANDOM FOREST REGRESSOR (RFR)

Random forest model is an ensemble method that combines multiple decision trees such that “each tree depends on the values of a random vector sampled independently and with the same distribution for all trees in the forest” [51]. We have trained the model with *numbers of trees* = 500. The rest of the parameters were: *criterion* = ‘mse’, *random-state* = 76, *max-features* = ‘auto’.

2) SUPPORT VECTOR REGRESSOR (SVR)

The support vector machines objective is to maximize the margin between the decision boundary (or separating hyperplane) and train the samples that are closest to the hyperplane. We used Radial Basis Function kernel (*RBF kernel*) to train the model. We used grid search and found the best parameters. The configuration of our SVR model is: *kernel* = ‘rbf’, *C* = 120, *gamma* = 0.0005.

3) MULTI-LAYER PERCEPTRON REGRESSOR (MLP-NN)

Multi-Layer Perceptron is supervised machine learning algorithm based on feed forward artificial neural network. The structure of the model is shown in Fig. 4. We trained the model with input layer containing 6 neurons, 2 hidden layers with 7 neurons and output layer with one neuron. The fully connected model was trained using *logistic* activation function with *learning rate* of 0.01 and 2000 *iterations*. The

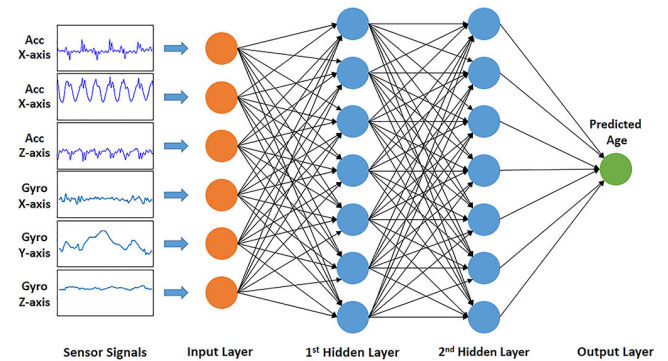


FIGURE 4. The structure of MLP Neural Network comprised of a fully connected network of 6 input neurons at input layer, 7 hidden neurons in each of the 2 hidden layers, and 1 output neuron in the output layer.

TABLE 3. List of all features extracted for each step from tri-axial accelerometer and tri-axial gyroscope sensors.

Feature	Acc	Gyr	Domain	Equation
Mean	x, y, z	–	Time	$\mu = \frac{1}{n} \sum_{i=1}^n X_i$
Median	x, y, z	–	Time	$[(n+1)/2]\text{th value}$
Maximum	x, y, z	x	Time	$\max(x)$
Minimum	x, y, z	x	Time	$\min(x)$
Root Mean Square	y, z	–	Time	$rms = \sqrt{\frac{1}{n} \sum_{i=1}^n X_i ^2}$
Index of Maximum	x, y, z	x	Time	Index of maximum value in step
Index of Minimum	–	x	Time	Index of minimum value in step
Power	y, z	–	Time	$pow = \frac{\sqrt{\sum_{i=1}^n X_i ^2}}{n}$
Energy	x, y	x, z	Time	$eng = \sum_{i=1}^n X_i ^2$
Entropy	–	z	Time	$ent = \sum_{i=1}^n (P_i) \log_2(P_i) \text{ where } P_i = \frac{\frac{S_i}{\max(S_i)}}{\sum_{i=1}^n \frac{S_i}{\max(S_i)}}$
Skewness	y, z	x	Time	$s = \frac{E(x-\mu)^3}{\sigma^3}$
Kurtosis	x, y, z	x, y	Time	$k = \frac{E(x-\mu)^4}{\sigma^4}$
Interquartile Range	–	x, y	Time	$iqr = Q_3 - Q_1 \text{ where } Q_1 = \frac{n}{4} \text{ and } Q_3 = \frac{3n}{4}$
Mean Absolute Deviation	x, y	y	Time	$mad = \frac{1}{n} \sum_{i=1}^n (X_i - \mu)$
Signal Magnitude Area	x	x	Time	$sma = \frac{1}{t} (\int_0^t x(t) dt + \int_0^t y(t) dt + \int_0^t z(t) dt)$
Band Power of Signal	x	x	Frequency	Average power in the signal, fft
Energy	–	x	Frequency	$eng_F = \sum_{i=1}^n fft_i ^2$
Magnitude	–	x	Frequency	$mag_F = \max(2 * fft)$
Mean	x	x, z	Frequency	$\mu_F = \frac{1}{n} \sum_{i=1}^n fft_i$

input of the network was 3D accelerometer and 3D gyroscope signals.

IV. RESULTS

All of the results were computed on a Jupyter Notebook with the following processing capabilities: CPU – Intel core i5, 2.4 GHz processor, RAM – 4GB, programming language – Python 3.6.1, Scikit-learn 0.19.1 [52]. For the evaluation purposes, the data were divided into three subsets: 1) Hybrid data consisting of data collected with both sensor modalities (smartphone embedded IMU, wearable IMU), 2) Smartphone data comprising of data collected with a smartphone's on-board MPU 6500 IMU, and 3) Wearable IMU data consisting of data collected with APDM Opal IMU. Stratified 10-fold cross validation and subject-wise cross validation were used to compare and evaluate estimators' performance. The results of both cross validation models were computed on complete data, gender restricted data, and age group restricted data. In the following two subsections, the results of stratified 10-fold cross validation and subject-wise cross validation are discussed.

A. 10-FOLD CROSS VALIDATION

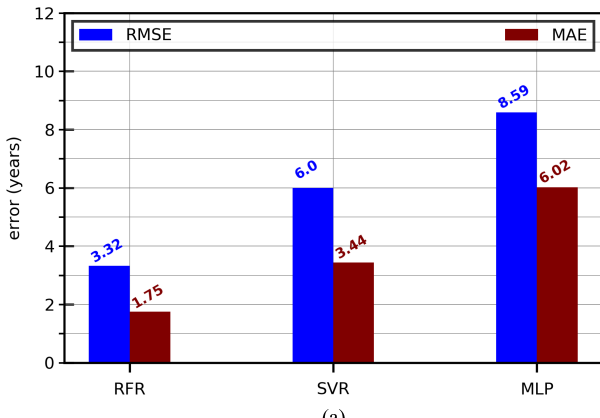
In this section, we present the outcomes of 10-fold cross validation model on each of the three datasets i.e. hybrid data, smartphone data, and wearable IMU data. The results are computed in root mean square error (RMSE) and mean absolute error (MAE) to evaluate and compare the performance of the three estimators.

1) HYBRID DATA

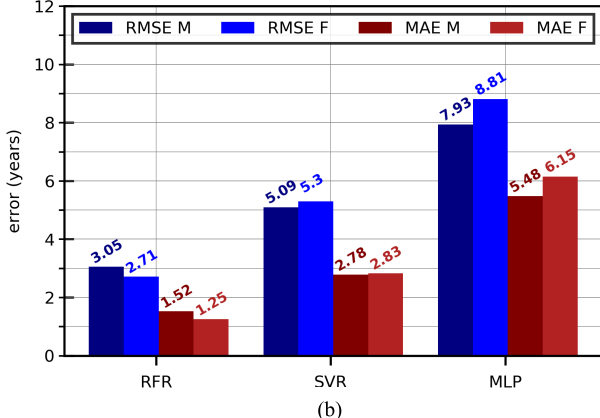
The results of age regression by each estimator on *complete data* (i.e. Setups A, B, C) are shown in Fig. 5(a). Lowest RMSE and MAE of 3.32 years and 1.75 years respectively are observed for RFR followed by SVR and MLP. The average RMSE (ascending order) is: RFR – 3.32 years, SVR – 6.0 years and MLP – 8.59 years. Whereas, the average MAE (ascending order) is: RFR – 1.75 years, SVR – 3.44 years and MLP – 6.02 years. In all of the cases, the p-value (<0.0001) is lower than the 5% statistical significance level.

For the case of gender restricted data, where the data are divided into two datasets i.e. male only and female only, the results are presented in Fig. 5(b). Again, lowest RMSE and MAE are seen for RFR followed by SVR and MLP in both male only data and female only data. For male only data, the average RMSE (ascending order) is: RFR – 3.05 years, SVR – 5.09 years and MLP – 7.93 years. Whereas, the average MAE (ascending order) is: RFR – 1.52 years, SVR – 2.78 years and MLP – 5.48 years. For female only data, the average RMSE (ascending order) is: RFR – 2.71 years, SVR – 5.3 years and MLP – 8.81 years. Whereas, the average MAE (ascending order) is: RFR – 1.25, SVR – 2.83 and MLP – 6.15 in years. The p-value (<0.0001) remains lower than the 5% statistical significance level in all of the cases.

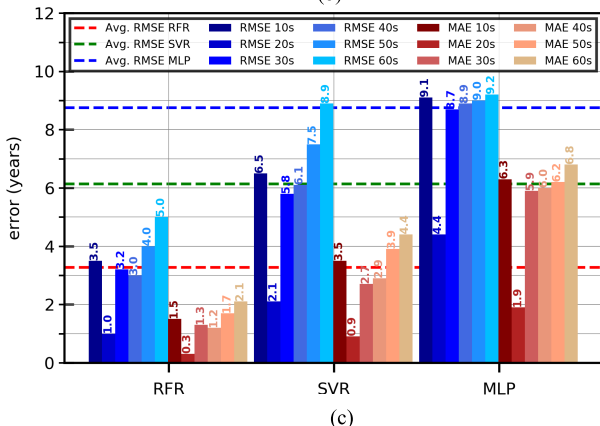
Fig. 5(c) shows the results of age regression on age group restricted data. Here we have divided the dataset into six age groups i.e. 10s (teenagers), 20s, 30s, 40s, 50s, 60s & above.



(a)



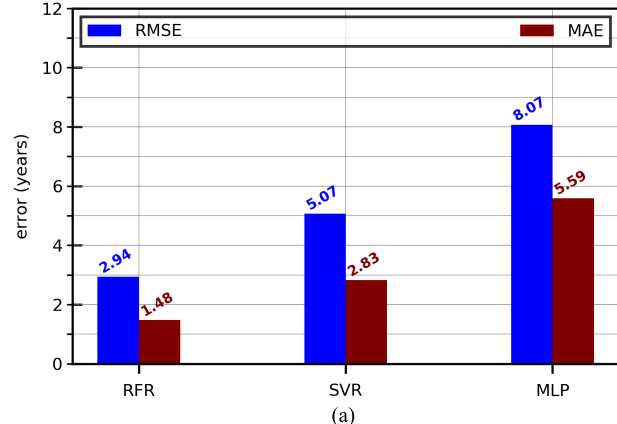
(b)



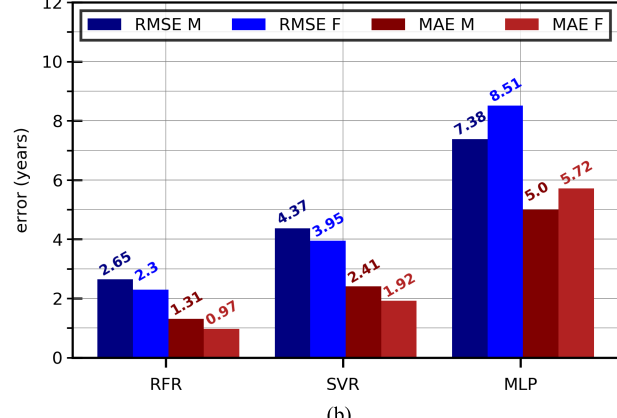
(c)

FIGURE 5. Results of 10-fold cross validation on hybrid data (smartphone embedded IMU + wearable IMU). The graphs present a comparison of root mean square (RMSE) and mean absolute error (MAE) for each case: (a) Complete data, (b) Gender restricted data case and (c) Age group restricted data.

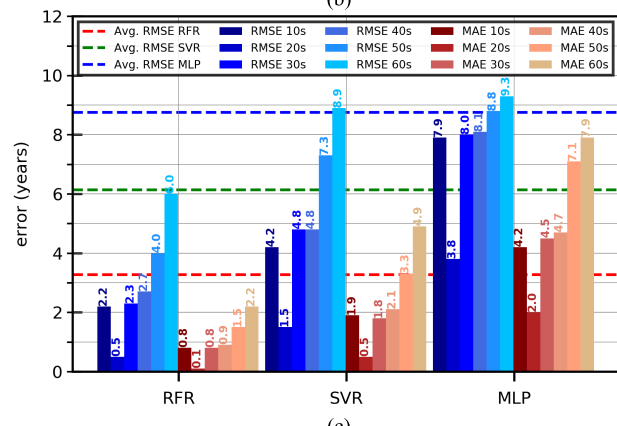
As observed earlier, lowest RMSE and MAE are produced by RFR followed by SVR and MLP and the p-value (<0.0001) stays lower than the 5% statistical significance level. The average RMSE (ascending order) is: RFR – 3.5, 1.0, 3.2, 3.0, 4.0 and 5.0 years, SVR – 6.5, 2.1, 5.8, 6.1, 7.5 and 8.9 years and MLP – 9.1, 4.4, 8.7, 8.9, 9.0 and 9.2 years for each age group respectively. Whereas, the average MAE (ascending order) is: RFR – 1.5, 0.3, 1.3, 1.2, 1.7 and 2.1 years, SVR – 3.5, 0.9, 2.7, 2.9, 3.9 and 4.4 years and MLP – 6.3, 1.9, 5.9, 6.0, 6.2, and 6.8 years for each age group respectively.



(a)



(b)



(c)

FIGURE 6. Results of 10-fold cross validation on data collected with a smartphone embedded MPU-6500. The graphs present a comparison of root mean square error (RMSE) and mean absolute error (MAE) for each case: (a) Complete data, (b) Gender restricted data and (c) Age group restricted data.

2) SMARTPHONE DATA

The results of age regression by each estimator on complete data (i.e. Setups A & B) collected through a smartphone's on-board IMU are shown in Fig. 6(a). RVR has outperformed SVR and MLP by producing lowest RMSE and MAE. The average RMSE (ascending order) is: RFR – 2.94 years, SVR – 5.07 years and MLP – 8.07 years. The average MAE (ascending order) is: RFR – 1.48 years, SVR – 2.83 years and MLP – 5.59 years. In all of the cases, the p-value (<0.0001) is lower than the 5% statistical significance level.

Fig. 6(b) shows the results of age regression by each estimator on gender restricted data. For male only data, the average RMSE (ascending order) is: RFR – 2.65 years, SVR – 4.37 years and MLP – 7.38 years. Whereas, the average MAE (ascending order) is: RFR – 1.31 years, SVR – 2.41 years, MLP – 5.0 years. For female only data, the average RMSE (ascending order) is: RFR – 2.3 years, SVR – 3.95 years, and MLP – 8.51 years. Whereas, the average MAE (ascending order) is: RFR – 0.97 years, SVR – 1.92 years, and MLP – 5.72 years. The p-value (<0.0001) stays lower than the 5% statistical significance level for all cases.

The bar graphs in Fig. 6(c) present the results of age regression on age group restricted data (10s, 20s, 30s, 40s, 50, 60s & above) by each estimator. Again, lowest RMSE and MAE are seen for RFR followed by SVR and MLP and the p-value (<0.0001) remains lower than the 5% statistical significance level. The average RMSE (ascending order) is: RFR – 2.2, 0.5, 2.3, 2.7, 4.0 and 6.0 years, SVR – 4.2, 1.5, 4.8, 4.8, 7.3 and 8.9 years and MLP – 7.9, 3.8, 8.0, 8.1, 8.8 and 9.3 years for each age group respectively. Whereas, the average MAE (ascending order) is: RFR – 0.8, 0.1, 0.8, 0.9, 1.5 and 2.2 years, SVR – 1.9, 0.5, 1.8, 2.1, 3.3 and 4.9 years and MLP – 4.2, 2.0, 4.5, 4.7, 7.1, and 7.9 years for each age group respectively.

The bar graphs in Fig. 7 present the setup-wise results of 10-fold cross validation on data collected through smartphone's on-board MPU-6500. In all cases, RFR produces lowest RMSE and MAE followed by SVR and MLP. For setup-A, the average RMSE (ascending order) remains: RFR – 2.16 years, SVR – 4.04 years and MLP – 5.98 years. The average MAE (ascending order) remains: RFR – 1.12 years, SVR – 2.22 years and MLP – 3.75. For setup-B, the average RMSE (ascending order) is: RFR – 3.72 years, SVR – 6.67 years and MLP – 10.8 years. The average MAE (ascending order) is: RFR – 1.86 years, SVR – 3.94 years and MLP – 8.69. For years. The p-value (<0.0001) is lower than the 5% statistical significance level in all of the cases.

3) WEARABLE IMU DATA

The results of age regression by each estimator on complete data collected through a wearable IMU (i.e. Setup-C) are presented in Fig. 8(a). RVR has outperformed SVR and MLP by producing lowest RMSE and MAE. However, for all estimators, both of the errors are higher as compared to the prediction errors computed on complete data collected with a smartphone. The average RMSE (ascending order) is: RFR – 5.42 years, SVR – 9.8 years, and MLP – 12.0 years. The average MAE (ascending order) is: RFR – 3.71 years, SVR – 6.95 years, and MLP – 10.2 years. The p-value (<0.0001) remains lower than the 5% statistical significance level for all of the results computed in this section.

The results of gender restricted data are shown in Fig. 8(b). As observed earlier, RVR outperforms SVR and MLP. For male only data, the average RMSE (ascending order) is: RFR – 5.27 years, SVR – 9.25 years and MLP – 13.1 years.

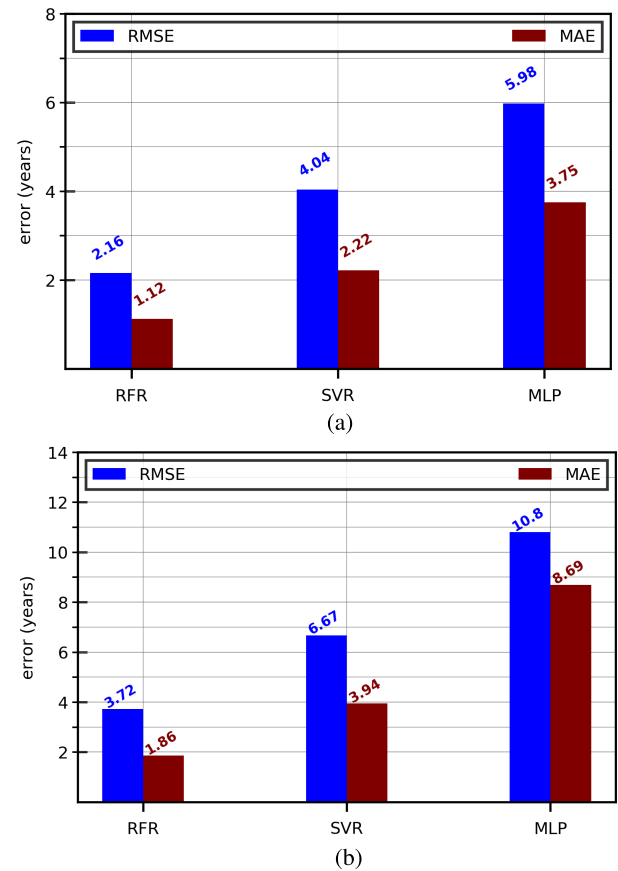


FIGURE 7. Results of 10-fold cross validation computed from the data collected under different data collection setups (Setup-A, Setup-B) using a smartphone embedded MPU-6500. RFR outperforms the rest of the predictors in all cases. (a) Setup-A. (b) Setup-B.

Whereas, the average MAE obtained (ascending order) is: RFR – 3.47 years, SVR – 6.22 years and MLP – 11.3 years. For female only data, the average RMSE (ascending order) is: RFR – 3.88 years, SVR – 6.98 years and MLP – 9.72 years. Whereas, the average MAE (ascending order) is: RFR – 2.33 years, SVR – 5.05 years and MLP – 7.8 years.

Fig. 8(c) presents the results of age regression on age group restricted data by each estimator. Again, lowest RMSE and MAE are seen for RFR followed by SVR and MLP. The average RMSE (ascending order) is: RFR – 6.2, 5.1, 3.6, 3.4 and 6.7 years, SVR – 12.2, 9.4, 6.3, 6.9 and 11.6 years and MLP – 12.4, 12.3, 10.2, 10.4 and 12.5 years for each age group respectively. Whereas, the average MAE (ascending order) is: RFR – 4.5, 3.3, 2.2, 2.1 and 4.6 years, SVR – 9.1, 6.5, 4.1, 4.5 and 8.9 years and MLP – 11.5, 11.2, 8.3, 8.6, and 11.6 years for each age group respectively.

B. SUBJECT WISE CROSS VALIDATION

The subject wise cross validation is derived from leave-one-out cross validation. Here all of the samples of one subject are left out and are reserved for testing whereas the rest of the samples are used for training. For n subjects, the process is repeated n times so that each subject is tested exactly once. The results are computed as RMSE on each of the three datasets i.e. hybrid data, smartphone data, and wearable

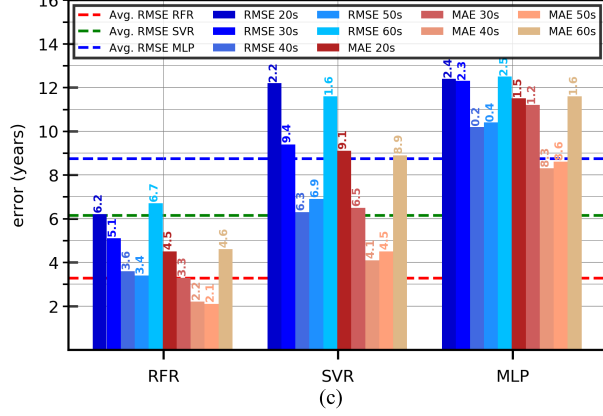
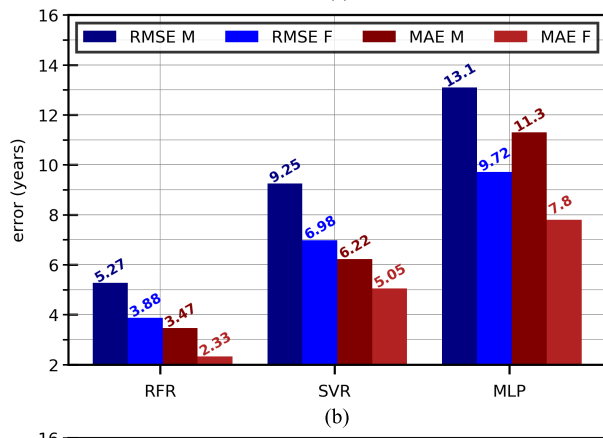
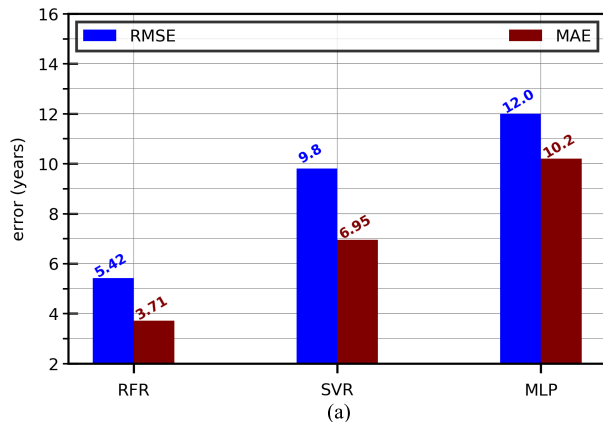


FIGURE 8. Results of 10-Fold cross validation on data collected with wearable IMU. The graphs present a comparison of root mean square error (RMSE) and mean absolute error (MAE) for each case: (a) Complete data, (b) Gender restricted data and (c) Age group restricted data In general, Random Forest Regressor outperforms other models.

IMU data. The results are visualized as a comparison between actual age and predicted age of subjects.

1) HYBRID DATA

The results of subject wise cross validation on complete data (i.e. Setups A, B, C) are presented in Fig. 9(a). The correlation is visually recognizable and lower age prediction error can be observed for age under 30 years. This is because of the fact that approximately 57% of the subjects in our database are below 30 years. The age prediction error is higher for underrepresented ages in the dataset and some outliers are

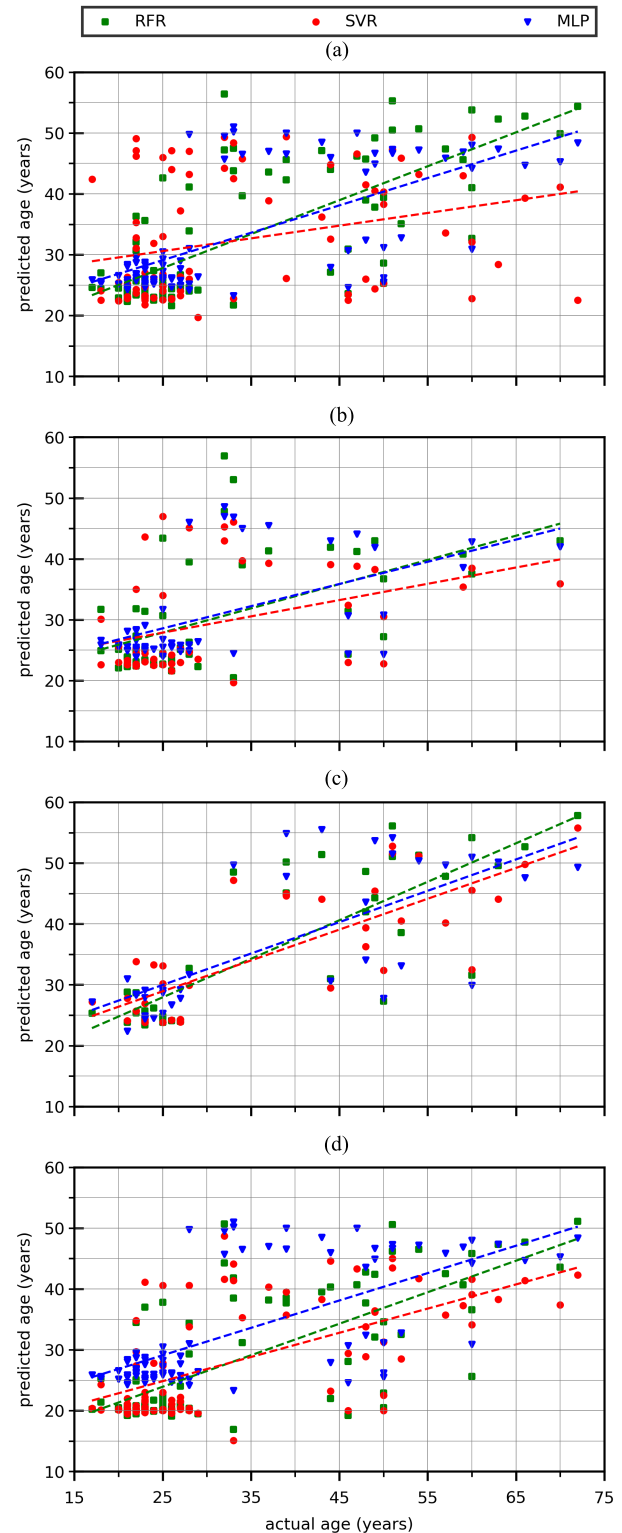


FIGURE 9. A comparison of actual age with predicted age computed during subject wise cross validation on hybrid data: RFR (square), SVR (circle), MLP (triangle). (a) Complete data, (b) Gender restricted data (male), (c) Gender restricted data (female), (d) Age group restricted data.

clearly observable. RFR predicts better than the rest of the models. The average RMSE (ascending order) is: RFR – 8.22 years, MLP – 8.75 years and SVR – 10.51 years.

In case of gender restricted data, for both male only and female only datasets, similar trends are observed where age prediction error is lower for age below 30 years and higher for the rest. The scatter plots of male data and female date are shown in Fig. 9(b) and (c) respectively. RFR has again outperformed the rest of the models and produced lower age prediction errors. The average RMSE (ascending order) for male only data is: MLP – 8.36 years, RFR – 8.49 years and SVR – 9.73 years. Whereas, the average RMSE (ascending order) for female only data is: RFR – 8.02 years, MLP – 9.78 years and SVR - 10.24 years.

When age group restriction is applied, a similar tendency is observed as shown in Fig. 9(d). The age prediction error is lower for age below 30 years and higher for the rest and the RFR outperformed SVR and MLP. The average RMSE (ascending order) is: RFR – 7.85 years, MLP – 8.71 years and SVR – 10.01 years.

2) SMARTPHONE DATA

Subject wise cross validation results computed with smartphone's complete data (i.e. Setups A & B), gender restricted data, and age group restricted data are presented in Fig. 10. In all of the cases and for all models, a tendency similar to hybrid data is observable where the predicted age error is lower for age below 30 years and higher for the underrepresented population. RFR is a better predictor than SVR and MLP as it produces lowest age prediction error for all datasets. The average RMSE (ascending order) computed on complete data are: RFR – 6.84 years, MLP – 7.28 years and SVR – 8.13 years. When gender restriction is applied on the data, the average RMSE (ascending order) computed on male only data is: RFR – 6.31 years, MLP – 6.59 years and SVR – 7.55 years. Whereas the average RMSE (ascending order) computed on female only data is: RFR – 6.70 years, SVR – 8.28 years and MLP – 9.06 years. On age group restricted data, the average RMSE (ascending order) is: RFR – 6.51 years, MLP – 7.29 years and SVR – 7.63 years.

Fig. 11 present the setup-wise results of subject wise cross validation on data collected through smartphone's on-board MPU-6500. When training and validating with the data of Setup-A only (Fig. 11(a)), the trend remains similar where the predicted age error remains lower for age below 30 years. This is due to the fact that the age of most of the subjects in Setup-A (around 92%) is below 30 years. The average RMSE (ascending order) is: RFR – 4.2 years, SVR – 5.07 years and MLP – 4.53 years. The results computed on the data of Setup-B are shown in Fig. 11b. The average RMSE remains higher i.e. RFR – 12.32 years, SVR – 13.85 years and MLP – 12.72 years. This is because of underrepresented population in Setup-B where the number of subjects are only 20 with an average age of 32.6 ± 13.7 years.

3) WEARABLE IMU DATA

Fig. 12 shows the results of subject wise cross validation computed on the wearable IMU's data, gender restricted data, and age group restricted data. The results are computed from the

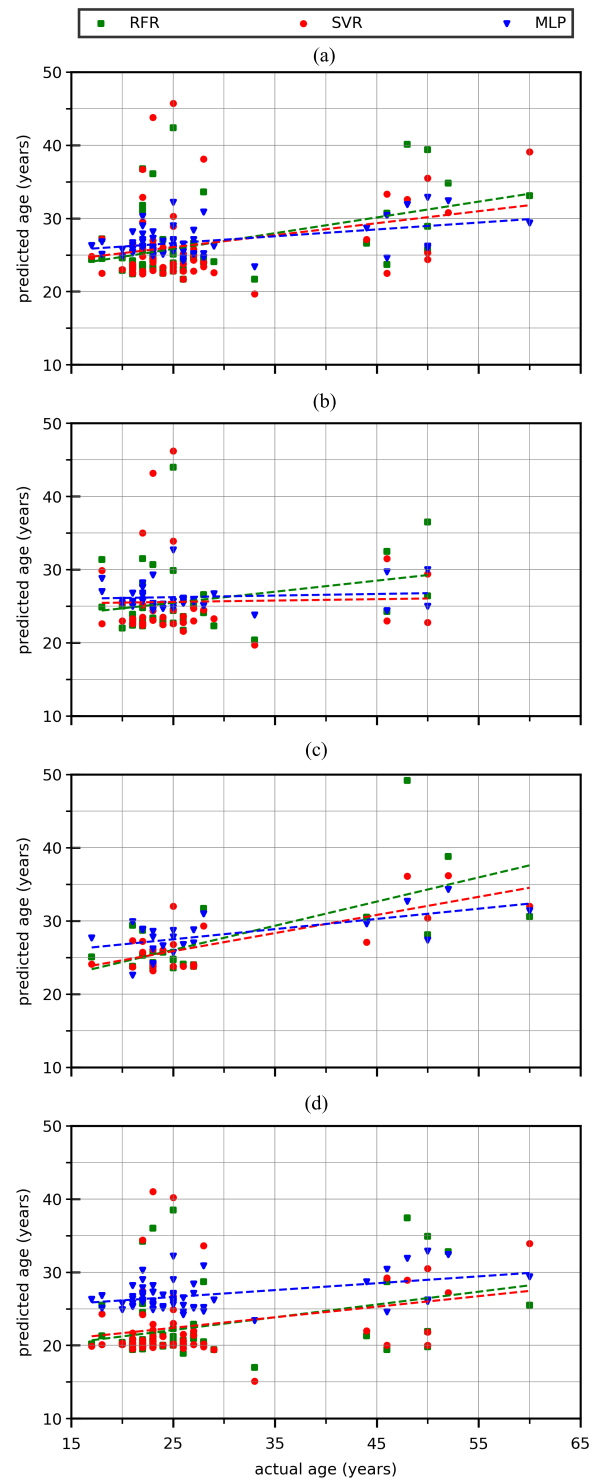


FIGURE 10. Scatter plots showing a comparison between actual age and predicted age computed during subject wise cross validation on smartphone data from different models: RFR (square), SVR (circle), MLP (triangle). (a) Complete data, (b) Gender restricted data (male), (c) Gender restricted data (female) (d) Age group restricted data.

data collected under Setup-C. Here, the trends are different from the previous two, because total number of participants in this dataset are 26 having an average age of 48.1 years. In case of complete data and age restricted data, RFR outperforms SVR and MLP. On the other hand, MLP outperforms RFR

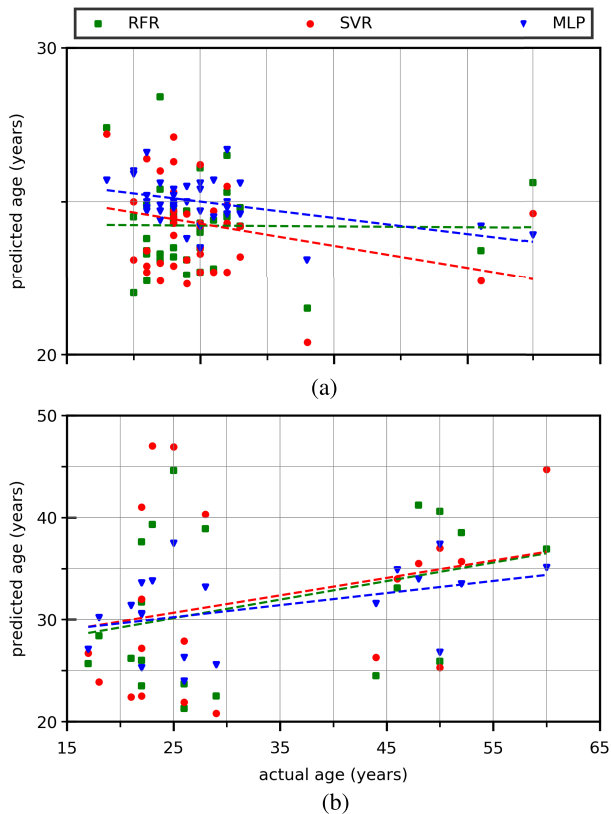


FIGURE 11. Scatter plots showing a comparison between actual age and predicted age computed by different models during subject wise cross validation on data collected under Setup-A and Setup-B: RFR (square), SVR (circle), MLP (triangle). (a) Setup-A. (b) Setup-B.

and SVR when gender restriction is applied on the data. However, the average RMSE is above 10 years for all datasets. The average RMSE (ascending order) on complete data is: RFR – 11.35 years, MLP – 11.82 years and SVR – 14.82 years. In case of gender restricted data, the average RMSE on male only data (ascending order) is: MLP – 14.92 years, RFR – 15.23 years and SVR – 16.26 years. Whereas, on female only data, the average RMSE (ascending order) is: MLP – 10.64 years, RFR – 10.7 years and SVR – 10.97 years. When age group restriction is applied, the average RMSE (ascending order) is: RFR – 10.67 years, MLP – 12.09 years and SVR – 14.22 years.

V. DISCUSSION

A. SUMMARY OF FINDINGS

The objective of the work at hand is to estimate chronological age of humans from the gait data of a single step recorded with a chest mounted IMU. For this purpose, we recorded human gait data represented by accelerations and angular velocities. We have used two different types of sensors i.e. smartphone embedded IMU (MPU-6500) and wearable IMU (APDM Opal) for data collection. The collected data itself is heterogeneous as it includes data from different ground surfaces, different human emotions, and the participants belong to two different demographical regions

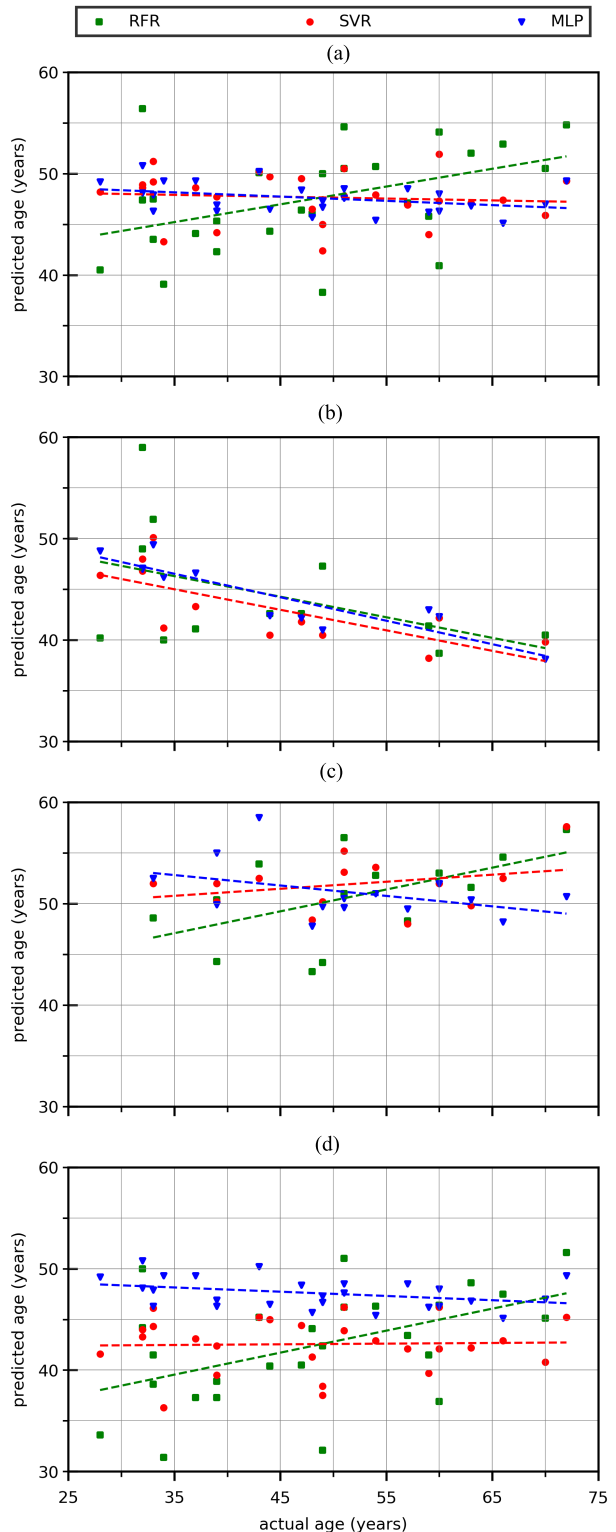


FIGURE 12. Scatter plots presenting a comparison between actual age and predicted age computed with subject wise cross validation on wearable IMU data from different models: RFR (square), SVR (circle), MLP (triangle). (a) Complete data, (b) Gender restricted data (male), (c) Gender restricted data (female) (d) Age group restricted data.

i.e. Europe and South-Asia. We have trained the models with three different estimators namely Random Forest, Support Vector Machines, and Multi-Layer Perceptron. For the

TABLE 4. Regression results obtained by 10-Fold Cross Validation (10-Fold CV) and Subject Wise Cross Validation (SW CV) for different categories: hybrid, smartphone and APDM Opal.

Category	Dataset	RMSE					
		RFR		SVR		MLP	
		10-Fold CV	SW CV	10-Fold CV	SW CV	10-Fold CV	SW CV
Hybrid Data	Complete Data	3.32	8.22	6.00	10.51	8.59	8.73
	Gender Restriction (Male)	3.05	8.49	5.09	9.73	7.93	8.36
	Gender Restriction (Female)	2.71	8.02	5.30	10.24	8.81	9.78
Smartphone Data	Age Group Restriction	3.27	7.85	6.14	10.01	8.75	8.71
	Complete Data	2.94	6.84	5.07	8.13	8.07	7.28
	Gender Restriction (Male)	2.65	6.31	4.37	7.55	7.38	6.59
APDM Opal Data	Gender Restriction (Female)	2.30	6.70	3.95	8.28	8.51	9.06
	Age Group Restriction	2.93	6.51	5.33	7.63	8.31	7.29
	Complete Data	5.42	11.35	9.80	14.82	12.0	11.82
APDM Opal Data	Gender Restriction (Male)	5.27	15.23	9.25	16.26	13.1	14.92
	Gender Restriction (Female)	3.88	10.70	6.98	10.97	9.72	10.64
	Age Group Restriction	4.99	10.67	9.27	14.22	11.6	12.09

purpose of cross validating predictions, 10-fold cross validation and subject wise cross validation were employed. The results have shown that reliable age estimation is possible with higher accuracy. On hybrid data (complete dataset), RFR has produced average RMSE of 3.32 years and MAE of 1.75 years for 10-fold cross validation model and average RMSE of 8.22 years when validated with subject wise cross validation model. Table 4 presents a detailed comparison of the average RMSE for different estimators, datasets, and validation strategies. It is observable that out of the three estimators evaluated in this study, random forest regressor has outperformed support vector regressor and multi-layer perceptron in most of the cases.

B. COMPARISON WITH EXISTING APPROACHES

Estimation of human soft biometrics including age is a key area of research and several methods of age estimation using non-visual features have been proposed. In one study, Kelishomi *et al.* [36] use smartphones to collect human walking data to classify age group and report an accuracy of 85%. Their approach is similar to the proposed approach, however, they only predict age groups instead of individual ages of subjects. A comparable methods is presented by Ahmed *et al.* [37] for classification of person age group using data collected with smartphone's on-board IMUs. They have achieved a classification accuracy of 94%. Riaz *et al.* [4] proposed a method of estimating human soft biometrics including gender, age, and height from gait data and report RMSE

of 11.51 years. Punyani *et al.* [53] used a feature set comprised of facial, gait and speech features to estimate person age. From facial features, they report an MAE of 5.36 years. While gait and speech features produce MAE of 6.57 and 6.62 years respectively. Hoffmann *et al.* [34] have used sensor floor to record gait data. They use MLP as estimator and report RMSE of 14.73 years and MAE of 9.55 years. However, their approach require special hardware and is limited to indoor environments only. In general, our approach produces lower RMSE and MAE than most of the existing approaches.

C. LIMITATIONS OF THE PROPOSED APPROACH

Our database consist of 86 different subjects with a male to female ratio of 49:37. The data consist of 252 minutes of recording including 1,134,000 frames and 19,614 steps. Moreover, most of the subjects (>50%) are under 30 years old. The participants belong to two demographically different regions, however, not in equal ratio resulting into unbalanced population. Hence, the presented results are a proof of concept only and further evaluation of the proposed approach with a larger database consisting of balanced population (in terms of age groups, demographical location of the subjects) will be considered in future work.

An evident limitation of our approach is sensor placement since we have only considered chest for sensor attachment. Other practical sensor placement locations such as wrists, lower back, ankles etc. should also be consider. This will help

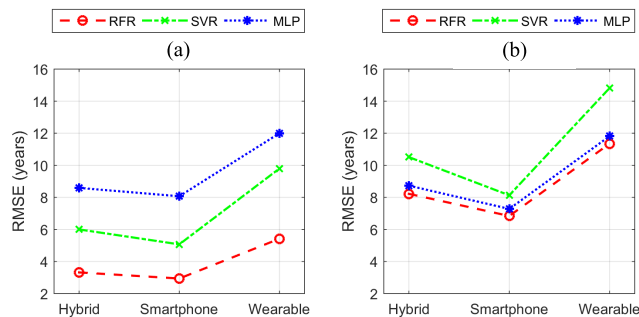


FIGURE 13. A comparison of RMSE computed by different estimators using (a) 10-fold CV and (b) subject wise CV on hybrid, smartphone, and wearable datasets. RFR produces lowest age prediction error in all cases.

in minimizing uncertainty in sensor placement and finding best locations with higher age prediction accuracy.

Another notable constraint of the proposed approach is the limited types of sensors used for data collection. We have used a smartphone's on-board IMU and a wearable IMU, however, this does not cover a wide range of sensors available in the market. Collecting further data with more low cost IMUs e.g. housed in smart watches, wrist bands, smart bracelets, smart shoes etc. and evaluating the proposed approach is another important area of future work.

For comparing the used techniques against deep learning methods (as have been used for age estimation from facial features [26], [54]) much larger collection of data are necessary. We will address such a comparison once larger bodies of data are available.

VI. CONCLUSION

The novelty of the presented work is finding a set of non-visual features (a total of 50 hand-crafted spatio-temporal features from 6D accelerations and angular velocities), which do not require heavy computational resources and which can be used to train a model to predict age of subjects with higher accuracy. We have compared three different estimator and found that random forest regressor is the most suitable estimator for the task of predicting human age as shown in Fig. 13. On hybrid data (collected with smartphone embedded IMU and wearable IMU), using complete dataset, the RFR has produced average RMSE of 3.32 years under 10-fold cross validation and 8.22 years under subject wise cross validation. In case of smartphone's MPU-6500 data only, while using complete dataset, the RFR has produced average RMSE of 2.94 years under 10-fold cross validation and 6.84 years under subject wise cross validation. When considering wearable IMU data only and using complete dataset, the average RMSE error produced by RFR is 5.42 years under 10-fold cross validation and 11.35 years under subject wise cross validation.

Despite the fact that our approach has certain limitations, the average age predication error is much lower than that of the existing methodologies [4], [34], [53]. It will be interesting to have longitudinal studies over several years or

even decades. The findings on the existing data point to change of gait while aging, which will also imply that person identification using gait depends on data that is not too old. Reliable and accurate estimates of age from the inertial sensors data of a smartphone raises several privacy concerns e.g. such estimates can be used for age group targeted online advertisements. Similarly, estimates of age along with other soft biometrics such as gender, height, and weight can be used for motion analysis of subjects. In this context, re-evaluating the proposed approach with larger datasets containing longer sequences of gait data collected with smart gadgets is an important direction for future work.

REFERENCES

- [1] M. P. Murray, "Gait as a total pattern of movement: Including a bibliography on gait," *Amer. J. Phys. Med. Rehabil.*, vol. 46, pp. 290–333, Feb. 1967.
- [2] N. Khamsemanan, C. Nattee, and N. Jianwattanapaisarn, "Human identification from freestyle walks using posture-based gait feature," *IEEE Trans. Inf. Forensics Security*, vol. 13, no. 1, pp. 119–128, Jan. 2018.
- [3] Z. Wu, Y. Huang, L. Wang, X. Wang, and T. Tan, "A comprehensive study on cross-view gait based human identification with deep CNNs," *IEEE Trans. Pattern Anal. Mach. Intell.*, vol. 39, no. 2, pp. 209–226, Feb. 2017.
- [4] Q. Riaz, A. Vögele, B. Krüger, and A. Weber, "One small step for a man: Estimation of gender, age and height from recordings of one step by a single inertial sensor," *Sensors*, vol. 15, pp. 31999–32019, Dec. 2015.
- [5] J. B. Flora, D. F. Lochtefeld, D. A. Bruening, and K. M. Iftekharuddin, "Improved gender classification using nonpathological gait kinematics in full-motion video," *IEEE Trans. Human-Machine Syst.*, vol. 45, no. 3, pp. 304–314, Jun. 2015.
- [6] K. Zhang et al., "Age group and gender estimation in the wild with deep RoR architecture," *IEEE Access*, vol. 5, pp. 22492–22503, 2017.
- [7] J. Lu and Y.-P. Tan, "Gait-based human age estimation," *IEEE Trans. Inf. Forensics Security*, vol. 5, no. 4, pp. 761–770, Apr. 2010.
- [8] J. Lu, G. Wang, and P. Moulin, "Human identity and gender recognition from gait sequences with arbitrary walking directions," *IEEE Trans. Inf. Forensics Security*, vol. 9, no. 1, pp. 51–61, Jan. 2014.
- [9] Y. H. Kwon and N. da Vitoria Lobo, "Age classification from facial images," in *Proc. IEEE Conf. Comput. Vis. Pattern Recognit.*, Jun. 1994, pp. 762–767.
- [10] J. Ylioinas, A. Hadid, and M. Pietikäinen, "Age classification in unconstrained conditions using LBP variants," in *Proc. 21st Int. Conf. Pattern Recognit. (ICPR)*, Nov. 2012, pp. 1257–1260.
- [11] M. T. B. Iqbal, M. Shoyaib, B. Ryu, M. Abdullah-Al-Wadud, and O. Chae, "Directional age-primitive pattern (DAPP) for human age group recognition and age estimation," *IEEE Trans. Inf. Forensics Security*, vol. 12, no. 11, pp. 2505–2517, Nov. 2017.
- [12] M. H. U. Rehman, C. S. Liew, T. Y. Wah, J. Shuja, and B. Daghighi, "Mining personal data using smartphones and wearable devices: A survey," *Sensors*, vol. 15, pp. 4430–4469, Feb. 2015.
- [13] D. Son et al., "Multifunctional wearable devices for diagnosis and therapy of movement disorders," *Nature Nanotechnol.*, vol. 9, no. 5, pp. 397–404, 2014.
- [14] W. Tao, T. Liu, R. Zheng, and H. Feng, "Gait analysis using wearable sensors," *Sensors*, vol. 12, no. 12, pp. 2255–2283, 2012.
- [15] A. Dutt. (May 9, 2018). NVIDIAVoice: AI-Powered Motion Capture: A Radical Step Toward Modern 3D Content Pipelines. Forbes. Accessed: Mar. 1, 2019. [Online]. Available: <https://www.forbes.com/sites/nvidia/2018/05/09/ai-powered-motion-capture-a-radical-step-toward-modern-3d-content-pipelines/>
- [16] K. H. T. Chu, X. Jiang, and C. Menon, "Wearable step counting using a force myography-based ankle strap," *J. Rehabil. Assistive Technol. Eng.*, vol. 4, p. 2055668317746307, Jan. 2017.
- [17] C. V. C. Bouten, K. T. M. Koekkoek, M. Verduin, R. Kodde, and J. D. Janssen, "A triaxial accelerometer and portable data processing unit for the assessment of daily physical activity," *IEEE Trans. Biomed. Eng.*, vol. 44, no. 3, pp. 136–147, Mar. 1997.
- [18] Q. Riaz, G. Tao, B. Krüger, and A. Weber, "Motion reconstruction using very few accelerometers and ground contacts," *Graph. Models*, vol. 79, pp. 23–38, May 2015.

- [19] J. Tautges *et al.*, "Motion reconstruction using sparse accelerometer data," *ACM Trans. Graph.*, vol. 30, pp. 18:1–18:12, May 2011.
- [20] N. Yodpijit, N. Tavichaiyuth, M. Jongprasithporn, C. Songwongamarit, and T. Sittiwanchai, "The use of smartphone for gait analysis," in *Proc. 3rd Int. Conf. Control Automat. Robot. (ICCAR)*, Apr. 2017, pp. 543–546.
- [21] L. Pepa, F. Verdini, and L. Spalazzi, "Gait parameter and event estimation using smartphones," *Gait Posture*, vol. 57, pp. 217–223, Sep. 2017.
- [22] R. J. Ellis *et al.*, "A validated smartphone-based assessment of gait and gait variability in parkinson's disease," *PLoS ONE*, vol. 10, no. 10, 2015, Art. no. e0141694.
- [23] B. Yoo, Y. Kwak, Y. Kim, C. Choi, and J. Kim, "Deep facial age estimation using conditional multitask learning with weak label expansion," *IEEE Signal Process. Lett.*, vol. 25, no. 6, pp. 808–812, Jun. 2018.
- [24] W. Pei, H. Dibeklioğlu, T. Baltrušaitis, and D. M. J. Tax. (Nov. 2017). "Attended end-to-end architecture for age estimation from facial expression videos." [Online]. Available: <https://arxiv.org/abs/1711.08690>
- [25] C. C. Ng, M. H. Yap, N. Costen, and B. Li, "Wrinkle detection using hessian line tracking," *IEEE Access*, vol. 3, pp. 1079–1088, 2015.
- [26] J. S. Kang, C. S. Kim, Y. W. Lee, S. W. Cho, and K. R. Park, "Age estimation robust to optical and motion blurring by deep residual CNN," *Symmetry*, vol. 10, p. 108, Apr. 2018.
- [27] R. R. Atallah, A. Kamsin, M. A. Ismail, S. A. Abdelrahman, and S. Zerdoumi, "Face recognition and age estimation implications of changes in facial features: A critical review study," *IEEE Access*, vol. 6, pp. 28290–28304, 2018.
- [28] Y. Liu, R. Collins, and Y. Tsin, "Gait sequence analysis using frieze patterns," in *Computer Vision—ECCV (Lecture Notes in Computer Science)*. Berlin, Germany: Springer, 2002, pp. 657–671.
- [29] M. Nabila, A. I. Mohammed, and B. J. Yousra, "Gait-based human age classification using a silhouette model," *IET Biometrics*, vol. 7, no. 2, pp. 116–124, 2018.
- [30] A. M. Sabatini, C. Martelloni, S. Scapellato, and F. Cavallo, "Assessment of walking features from foot inertial sensing," *IEEE Trans. Biomed. Eng.*, vol. 52, no. 3, pp. 486–494, Mar. 2005.
- [31] K. Ellis, J. Kerr, S. Godbole, J. Staudemayer, and G. Lanckriet, "Hip and wrist accelerometer algorithms for free-living behavior classification," *Med. Sci. Sports Exerc.*, vol. 48, no. 5, p. 933, 2016.
- [32] A. Mannini and A. M. Sabatini, "Accelerometry-based classification of human activities using Markov modeling," *Comput. Intell. Neurosci.*, vol. 2011, p. 4, Jan. 2011.
- [33] G. Dobry, R. M. Hecht, M. Avigal, and Y. Zigel, "Supervector dimension reduction for efficient speaker age estimation based on the acoustic speech signal," *IEEE Trans. Audio, Speech, Language Process.*, vol. 19, no. 7, pp. 1975–1985, Sep. 2011.
- [34] R. Hoffmann, C. Lauterbach, J. Conradt, and A. Steinhage, "Estimating a person's age from walking over a sensor floor," *Comput. Biol. Med.*, vol. 95, pp. 271–276, Apr. 2018.
- [35] I. Tsimperidis, S. Rostami, and V. Katos, "Age detection through keystroke dynamics from user authentication failures," *Int. J. Digit. Crime Forensics*, vol. 9, no. 1, pp. 1–16, 2017.
- [36] A. E. Kelishomi, Z. Cai, and M. H. Shayesteh, "Tracking user information using motion data through smartphones," in *Proc. IEEE Int. Joint Conf. Biometrics (IJCB)*, Oct. 2017, pp. 286–293.
- [37] U. Ahmed, M. F. Ali, K. Javed, and H. A. Babri. (2017). "Predicting physiological developments from human gait using smartphone sensor data." [Online]. Available: <https://arxiv.org/abs/1712.07958>
- [38] S. Wan, Y. Liang, Y. Zhang, and M. Guizani, "Deep multi-layer perceptron classifier for behavior analysis to estimate Parkinson's disease severity using smartphones," *IEEE Access*, vol. 6, pp. 36825–36833, 2018.
- [39] G. M. Weiss and J. W. Lockhart, "Identifying user traits by mining smart phone accelerometer data," in *Proc. 5th Int. Workshop Knowl. Discovery Sensor Data*, 2011, pp. 61–69.
- [40] A. R. Alharbi and M. A. Thornton, "Demographic group prediction based on smart device user recognition gestures," in *Proc. 15th IEEE Int. Conf. Mach. Learn. Appl. (ICMLA)*, Dec. 2016, pp. 100–107.
- [41] Y. Sun, M. Zhang, Z. Sun, and T. Tan, "Demographic analysis from biometric data: Achievements, challenges, and new frontiers," *IEEE Trans. Pattern Anal. Mach. Intell.*, vol. 40, no. 2, pp. 332–351, Feb. 2018.
- [42] X. Geng, Z.-H. Zhou, and K. Smith-Miles, "Automatic age estimation based on facial aging patterns," *IEEE Trans. Pattern Anal. Mach. Intell.*, vol. 29, no. 12, pp. 2234–2240, Dec. 2007.
- [43] H. Han, C. Otto, and A. K. Jain, "Age estimation from face images: Human vs. Machine performance," in *Proc. Int. Conf. Biometrics (ICB)*, Jun. 2013, pp. 1–8.
- [44] X. Wang, R. Guo, and C. Kambhamettu, "Deeply-learned feature for age estimation," in *Proc. IEEE Winter Conf. Appl. Comput. Vis. (WACV)*, Jan. 2015, pp. 534–541.
- [45] G. Levi and T. Hassner, "Age and gender classification using convolutional neural networks," in *Proc. IEEE Conf. Comput. Vis. Pattern Recognit. Workshops*, Jun. 2015, pp. 34–42.
- [46] InvenSense. *MPU-6500 MEMS MotionTracking Devices*. Accessed: Jul. 10, 2018. [Online]. Available: <https://www.invensense.com/products/motion-tracking/6-axis/mpu-6500/>
- [47] A. Opal. *Wireless, Wearable, Synchronized Inertial Measurement Units (IMUs) | APDM*. Accessed: Jul. 10, 2018. [Online]. Available: <http://www.apdm.com/wearable-sensors/>
- [48] F. Li, C. Zhao, G. Ding, J. Gong, C. Liu, and F. Zhao, "A reliable and accurate indoor localization method using phone inertial sensors," in *Proc. ACM Conf. Ubiquitous Comput. (UbiComp)*, New York, NY, USA, 2012, pp. 421–430.
- [49] M. O. Derawi, C. Nickel, P. Bours, and C. Busch, "Unobtrusive user-authentication on mobile phones using biometric gait recognition," in *Proc. 6th Int. Conf. Intell. Inf. Hiding Multimedia Signal Process.*, Oct. 2010, pp. 306–311.
- [50] W. Zijlstra, "Assessment of spatio-temporal parameters during unconstrained walking," *Eur. J. Appl. Physiol.*, vol. 92, nos. 1–2, pp. 39–44, Jul. 2004.
- [51] L. Breiman, "Random forests," *Mach. Learn.*, vol. 45, no. 1, pp. 5–32, 2001.
- [52] F. Pedregosa *et al.*, "Scikit-learn: Machine learning in Python," *J. Mach. Learn. Res.*, vol. 12, pp. 2825–2830, Oct. 2011.
- [53] P. Punyani, R. Gupta, and A. Kumar, "A comparison study of face, gait and speech features for age estimation," in *Advances in Electronics, Communication and Computing*. Singapore: Springer, 2018, pp. 325–331.
- [54] R. Rothe, R. Timofte, and L. Van Gool, "Deep expectation of real and apparent age from a single image without facial landmarks," *Int. J. Comput. Vis.*, vol. 126, pp. 144–157, Apr. 2018.



QAISE RIAZ received the Ph.D. (Dr. rer. nat.) degree in computer science from the University of Bonn, Germany, in 2016, and the M.S. degree in autonomous systems from the Bonn-Rhein-Sieg University of Applied Sciences, Sankt Augustin, Germany, in 2011.

Since 2016, he has been an Assistant Professor with the Department of Computing, School of Electrical Engineering and Computer Science, National University of Sciences and Technology, Islamabad, Pakistan. His research interests include motion capturing, human motion analysis and synthesis using low-cost sensors, character animation, and machine learning.



MUHAMMAD ZEESHAN UL HASNAIN HASHMI received the M.C.S. degree in computer science from the COMSATS Institute of Information Technology, Wah Cantonment, Pakistan, in 2016. He is currently pursuing the M.S. degree in computer science with the Department of Computing, School of Electrical Engineering and Computer Science, National University of Sciences and Technology, Islamabad, Pakistan.

His research interests include the human motion analysis, inertial-based motion analysis, and ubiquitous computing. He received the Institute and Campus Gold Medal from the COMSATS Institute of Information Technology, in 2016.



MUHAMMAD ARSLAN HASHMI received the M.C.S. degree from the COMSATS Institute of Information Technology, Wah Cantonment, Pakistan, in 2016. He is currently pursuing the M.S. degree in computer science with the Department of Computing, School of Electrical Engineering and Computer Science, National University of Sciences and Technology, Islamabad, Pakistan.

His research interests include the inertial-based human motion analysis and ubiquitous computing. In 2016, he received the Institute and the Campus Silver Medal from the COMSATS Institute of Information Technology.



MUHAMMAD SHAHZAD received the B.E. degree in electrical engineering from the National University of Sciences and Technology, Islamabad, Pakistan, in 2004, the M.S. degree in autonomous systems from the Bonn-Rhein-Sieg University of Applied Sciences, Sankt Augustin, Germany, in 2011, and the Ph.D. degree in radar remote sensing and image analysis from the Department of Signal Processing in Earth Observation (SiPEO), Technische Universität München (TUM), Munich, Germany, in 2016. He attended twice two weeks professional thermography training course at the Infrared Training Center, North Billerica, MA, USA, in 2005 and 2007, respectively.

He was a Visiting Research Scholar with the Institute for Computer Graphics and Vision, Technical University of Graz, Austria. Since 2016, he has been a Senior Researcher with SiPEO, TUM, Germany, and an Assistant Professor with the School of Electrical Engineering and Computer Science, National University of Sciences and Technology. His research interests include deep learning, object detection, image classification, processing unstructured/structured 3-D point clouds, optical RGBD data, and very high-resolution radar images.



HASSAN ERRAMI received the Ph.D. (Dr. rer. nat.) degree in mathematics from the University of Kassel, Germany, in 2013, and the M.S. degree in computer science from the University of Bonn, Germany, in 2008.

Since 2010, he has been a member of the research group Multimedia, Simulation and Virtual Reality, Institute for Computer Science, University of Bonn. His research interests include motion analysis and synthesis, sonification, and mathematical/computational models in system biology.



ANDREAS WEBER received the degree in mathematics and computer science from the Universities of Tübingen, Germany, and Boulder, CO, USA, and the M.S. (Dipl.-Math) degree in mathematics and the Ph.D. (Dr. rer. nat.) degree in computer science from the University of Tübingen, in 1990 and 1993, respectively.

From 1995 to 1997, he was a Postdoctoral Fellow with Cornell University. From 1997 to 1999, he was a member of the Symbolic Computation Group, University of Tübingen, Germany. From 1999 to 2001, he was a member of the research group Animation and Image Communication, Fraunhofer Institute for Computer Graphics. Since 2001, he has been a Professor of computer science with the University of Bonn, Germany.

• • •